

Cosmic ray anisotropies to 5 PeV

A. D. Erlykin ^{1,2} and A. W. Wolfendale ²

(1) P N Lebedev Physical Institute, Moscow, Russia

(2) Department of Physics, Durham University, Durham, UK

June 19, 2018

Abstract

Several large cosmic ray (CR) detectors have recently provided data on the arrival directions of CR, which taken together with previous data recorded over many decades allow the amplitude and phase of the first harmonic to be derived with reasonable precision and up to higher energies. We find a high degree of consistency amongst the various measurements. The new data indicate that at an energy above ~ 0.1 PeV a change of the CR anisotropy sets in. The amplitude of the first harmonic, which rises to 3 TeV, then diminishes and begins to rise again. The direction of the phase also changes to the opposite one. A measure of understanding follows from the use of two-dimensional maps of cosmic ray excesses over the mean background. When the energy of cosmic rays approaches the PeV region, the excess of cosmic rays moves from the Galactic Anti-Centre to the opposite direction of the Galactic Centre. The possible role of such potential cosmic ray sources as the supernovae Monogem Ring and Vela, which could help to explain some of the observed results, is discussed.

1 Introduction

It is very well known that the biggest problem in the quest to find the origin of CR is the presence of magnetic fields in the Interstellar Medium (ISM). The fields have both regular and irregular components and both play a role in causing the CR to travel by torturous paths. The irregular component, which dominates, causes the CR to effectively diffuse from their sources.

The present work comprises a quick survey of the results on CR anisotropies which, hopefully, have relevance to the origin problem, together with the necessary information about the mode of transport of the CR, specifically the regular and irregular field properties. Particular emphasis is given to the new data at sub-PeV and PeV energies which appeared since our latest paper on this subject [1].

A particular quest is to see if there is evidence favouring our 'Single Source Model' (SSM) (see [2] and later papers), in which a particular supernova remnant (SNR) (presumed to be the Monogem Ring) is the main cause of the sharp knee in the CR energy spectrum at about 3-4 PeV. According to our model a change in anisotropy

and phase might be expected at energies approaching 1 PeV. A similar scenario has been invoked by Sveshnikova et al. (2011) [3] in terms of one or more local SNR being responsible for some, at least, of the 'fine structure' of CR energy spectra and the form of the declination (δ) versus right ascension (RA) plots. Also included in the analysis is a study of the anisotropy of the lower energy CR, i.e. from $\log E = 2$ to $\log E = 5$, where E is in GeV.

2 The measured cosmic ray anisotropies

2.1 Hazards in measuring the anisotropies

In principle, the CR intensity will be a complicated function of Galactic longitude and latitude (ℓ, b) or, equivalently, right ascension and declination (RA, δ). It is customary, and reasonable, however, to represent it by two components. The first is in terms of a simple flow - with a near-sinusoidal intensity variation, in a fixed declination band (insofar as the detectors sweep out a band of constant declination). This gives the anisotropy amplitude A , and the phase in RA . The second is the residual excess, or excesses, which remain after the first harmonic has been subtracted.

When only a limited declination range is available, the measured value of A has to be corrected to allow for the fact that the declination at which the CR maximum is detected is not necessarily the centre of the declination range available for study. This point was made by Kiraly et al. (1979) [4] and very recently by Lidvansky et al. (2012) [5].

Even in the past, when only measurements of the counting rate (as, for example, with neutron monitors) were used for the study of anisotropy, or the arrival directions of CR particles were measured with a large uncertainty (muon telescopes), it was noted that the use of just the first harmonic was not enough to get a good fit of the CR spatial variation. The use of two harmonics improves the fit, but it means that the spatial distribution of the CR intensity has a rather complicated structure. Nowadays, when the arrival directions of the CR particles are measured with good accuracy, the constructed two-dimensional maps of the CR intensity have confirmed the complicated structure of the CR sky and allowed its analysis on different angular scales.

2.2 Summary of the amplitudes and phases of the first harmonics

Figure 1 shows a summary of the estimates of amplitude and phase derived from a number of previous summaries, specifically [1] (to be referred to as EW1). This new summary includes the latest data from Super-Kamiokande [6], MILAGRO [7], ARGO-YBJ [8], IceCube [9] and IceTop [10], as well as updated data from EAS-TOP [11], which were not shown in our previous summary EW1. The errors of the amplitudes and phases of these latest works are shown as they are given by the authors, except for IceTop, about which we shall comment later.

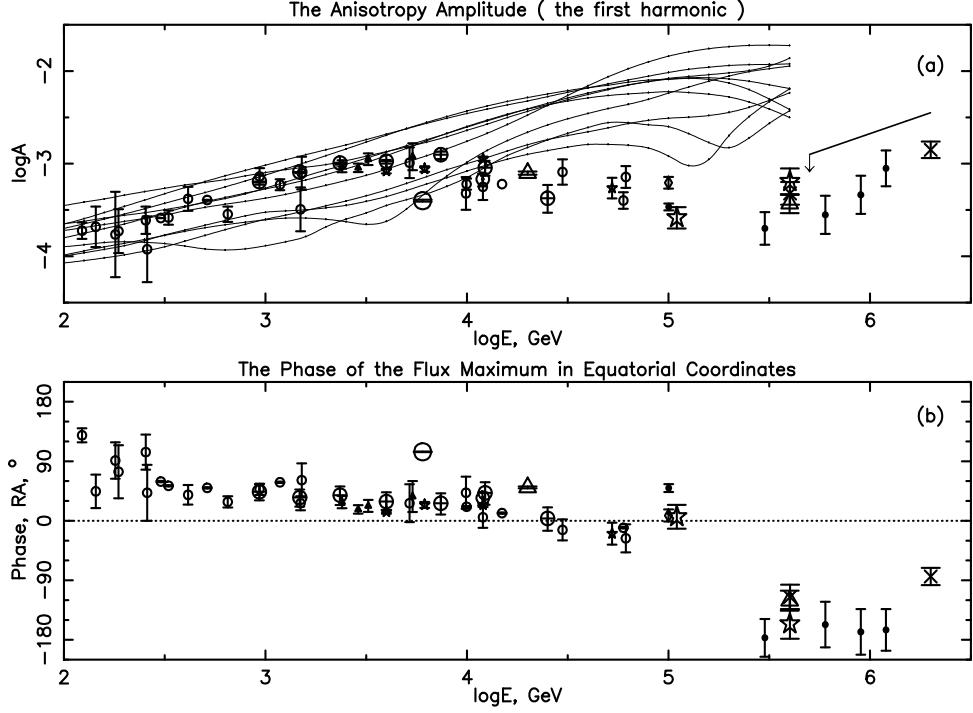


Figure 1: The observed amplitude (a) and the equatorial phase (b) of the first harmonic of the CR anisotropy. The bulk of the data were taken from Figure 5 of our previous survey EW1. The new data are denoted as \odot - Super-Kamiokande [6], \bigcirc - MILAGRO [7], \oplus - ARGO-YBJ [8], \star - updated EASTOP [11], \triangle - IceCube [9], \times - IceTop [10]. Thin full lines - the calculations for 10 different configurations of SNR including a single source which is tentatively associated with the Monogem Ring SNR [1].

The IceCube measurements cover the energy range from tens to hundreds of TeV [9]. The distribution of primary energies responsible for the production of the detected TeV muons is rather wide. The median energies for two selected energy bands are 0.02 and 0.4 PeV. It can be remarked that in this energy range the amplitude of the first harmonic falls down from $(0.79 \pm 0.01_{stat} \pm 0.03_{syst}) \cdot 10^{-3}$ to $(0.37 \pm 0.07_{stat} \pm 0.07_{syst}) \cdot 10^{-3}$ and the phase changes from $50.5 \pm 1.0_{stat} \pm 1.1_{syst}$ degrees to $-120.8 \pm 10.6_{stat} \pm 10.8_{syst}$ degrees.

The IceTop measurements cover the range of higher energies [10]. The median values rise from 0.4 PeV to 2 PeV and at the lower energy band they overlap with IceCube data giving the possibility to make a comparison between two independent experiments carried out at the same location at the South Pole and covering the same primary energies. However, a direct comparison of the published results is not possible. The IceTop collaboration prefers to fit their intensity profile by the superposition of a flat background and a 'gaussian' dip. In order to make the comparison with IceCube and other works we fitted the IceTop profile with the traditional two-harmonic function. The result of the best fit for both 0.4 PeV and 2 PeV energy domains is given in Table 1 and shown in Figure 1 for the first harmonic.

Table 1

Anisotropy amplitude and phase for two energy domains in IceTop

E^{med}, PeV	$A_1(10^{-3})$	$RA_1(\text{deg})$	$A_2(10^{-3})$	$RA_2(\text{deg})$	χ^2/ndf
0.4	0.48 ± 0.16	245 ± 19	0.39 ± 0.15	0.72 ± 1.12	26.5/14
2.0	1.41 ± 0.32	276 ± 13	-0.69 ± 0.32	257 ± 13	7.1/14

It is seen that in the 0.4 PeV energy band, where both IceCube and IceTop measurements overlap, there is good agreement between the amplitudes and phases of the anisotropy in both experiments, which gives some measure of credibility for their results at lower and higher energies. IceTop data indicate that in the PeV region the amplitude of the first harmonic starts to rise and also the phase is changing.

Recent measurements of the anisotropy in the Northern Hemisphere were made by Super-Kamiokande [6], MILAGRO [7], ARGO-YBJ [8] and the updated EAS-TOP data [11]. They did not reach the energy region above 0.1 PeV, but are useful because they are complementary to the measurements in the Southern Hemisphere and give the possibility of building a global map of the CR sky.

In EW1 we have already used the preliminary data from Super-Kamiokande. Their final data, as well as data from MILAGRO, ARGO-YBJ, although obtained at slightly lower energies with the median value of 6-10 TeV agree well with the IceCube data at 20 TeV. It gives the opportunity to claim that excess and dip regions cover a very broad range of declinations at tens of TeV energies.

Keeping in mind that the harmonic fit does not give a good description of the observed anisotropy, we, nevertheless, consider that the change in the energy dependence of the amplitude and phase, which occurs at energies above ~ 0.1 PeV and was first noticed by the EASTOP collaboration [11], is confirmed by the latest measurements and therefore worthy of interpretation.

The change of the amplitude and phase which occurs as the primary energy approaches the PeV region, with the well known knee at 3-4 PeV, supports the astrophysical origin of the knee and allows us to discount the nuclear physics model, in which the knee is caused by a change of the interaction characteristics of the primary CR particles with air nuclei.

Before continuing mention should be made of the remarkable 20 degree-radius excesses observed by MILAGRO and Tibet. Heliospheric phenomena are a distinct possibility, or very local ISM irregularities, although an explanation in terms of EAS initiated by gamma rays from distant discrete sources cannot be ruled out.

At this stage it is necessary to describe the objectives of the present work, specifically. They are as follows.

- (i) To interpret the A, ϕ values up to $\log E, \text{GeV} = 5$, i.e. why the amplitude and phase should be nearly energy independent and why the values are as measured.
- (ii) To interpret the values beyond $\log E, \text{GeV} = 5$, in terms of a single source, or otherwise.

3 Interpretation of the anisotropies below $\log E = 5$

3.1 Initial examination of the observations and comparison with prediction

It is evident from Figure 1a that there is consistency between the various sets of data - a welcome result in Cosmic Ray Physics. A mean line has a slow increase in $\log A$ with increasing energy to a maximum at about $\log E, GeV = 3.5$. A slow fall follows to a minimum at about $\log E, GeV = 5.5$.

The actual degree of consistency for the amplitudes from one experiment to another has been examined in two ways: by studying the dispersion in amplitudes ($\log A$) about the smooth line and by doing likewise in terms of the number of standard deviations from the line for each experimental data point. The 'smooth line' is simply a line through the unweighted averages of the values for half-decadal energy ranges with no overlap, it is not shown so as not to confuse the Figure 1, but it can be easily visualised. The result for the former is that the median displacement of the points from the line is $\Delta \log A = 0.1$, with 5% beyond $\Delta \log A = 0.3$. For the standard deviations σ , the median is 0.08σ , with 5% beyond 3σ , a somewhat higher percentage than expected for a Gaussian, but not dramatically so.

The former shows that the 'curvature' in $\log A$ vs $\log E$, with a peak at about $\log E, GeV = 3.5$ higher than the mean of the values of $\log A$ at $\log E = 2.0$ and 5.0 by $\Delta \log A = 0.6$, is genuine. The latter gives confirmation.

Turning to the phases, for absolute values the median dispersion is $\sim 10^\circ$ with 5% greater than 60° . In terms of the number of standard deviations, the method cannot be used because in one third of the points errors are difficult to read from the original figures. Nevertheless, the dispersion of the phase, as such, gives no cause for claiming other than a straight line for $\log(RA)$ vs $\log E$: there is no large scale feature mirroring the curvature in $\log A$. The significance of this result will be considered later.

Concerning our prediction (thin lines in Figure 1a [1]), there is modest agreement between our mean and the observations to $\log E, GeV \approx 3.5$ but an increasing discrepancy above. A change must be made to the model. Two possibilities are considered:

- (i) There is a Giant Galactic Halo
- (ii) The CR lifetime at high energies falls down more slowly with rising energy than it does at low energies

3.2 The amplitude of the anisotropy

3.2.1 A Giant Galactic Halo

We start with a suggestion to invoke a Giant Galactic Halo (GGH) having the uniform spatial distribution at least within the Galactic Disc and diffusive properties different from those in the conventional '1kpc Halo'. Since the uniform spatial distribution means complete isotropy with $A = 0$ the contribution of the GGH to the total CR flux would help to understand the low value of the anisotropy.

The presence of such a Halo has received important support very recently from the

Chandra X-ray Observatory [12]. The observations indicate a Giant Halo of radius over 100kpc, mean temperature $(1 - 2.5) \cdot 10^6 \text{K}$ and total mass of $\sim 10^{11} M_{\odot}$. The energy density of the plasma is thus 0.15 to 0.4 eVcm^{-3} , close to that in CR in the Galactic Disc.

Empirically, the average of the predicted $A(E)$ samples in Figure 1a exceeds the observed amplitudes at $\log E, \text{GeV} \approx 5.0 - 5.5$ by a factor of about 20. This would mean that at these energies some 95% of the CR come from the GGH. If the CR energy spectrum in the GGH is steeper than that in the Galactic Disc then at smaller energies the fraction of CR from the Disc would be smaller still.

The cause of the steeper energy spectrum of particles in the GGH could, in principle, be the existence of the Galactic Wind which carries away low energy particles from the Galactic Disc to the GGH. However, simple calculations of the particle balance in the system of Galactic Disc, Giant Galactic Halo and Extragalactic Space shows that if this system is in dynamic equilibrium, the GGH is not affected by the Galactic Wind. The preservation of the particle balance means that the particle input to the Disc from SN explosions has to be equal to the particle output from the Halo into Extragalactic Space. The equations are similar to those used in the leaky box model:

$$N^d(E)/\tau^d(E) + N^d(E)f/\tau^w(E) = Q(E) = N^h(E)/\tau^h(E) \quad (1)$$

Here, $N^d(E)$, $N^h(E)$ are energy spectra of particles in the Disc and Halo, $\tau^d(E)$, $\tau^w(E)$, $\tau^h(E)$ are lifetimes of particles in the Disc, Wind and Halo respectively and $Q(E)$ is the spectrum of particles injected by SNR into the Disc. The second term in the equation takes into account the output spectrum of particles carried away by the Wind. It is presented as the fraction of the Disc particles f and the energy dependence of this fraction is included into the lifetime $\tau^w(E)$.

If, for example, all energy dependencies in (1) are of the power law type, ie

$$Q(E) = Q_0 \left(\frac{E}{E_0}\right)^{-\gamma_{inj}}; \tau^{d,w,h}(E) = \tau_0^{d,w,h} \left(\frac{E}{E_0}\right)^{-\delta^{d,w,h}}; \quad (2)$$

then the solutions of the equations (1) are

$$N^d(E) = \frac{Q_0 \tau_0^d (E/E_0)^{-(\gamma_{inj} + \delta^d)}}{1 + \frac{f \tau_0^d}{\tau_0^w} (E/E_0)^{-(\delta^d - \delta^w)}} \quad (3)$$

$$N^h(E) = Q_0 \tau_0^h (E/E_0)^{-(\gamma_{inj} + \delta^h)} \quad (4)$$

As an example we present the solution of equations (3) and (4) in Figure 2 for the numerical values shown in Table 2:

Object	τ_0, year	δ
Halo	$4 \cdot 10^9$	0.6
Disc	$4 \cdot 10^7$	0.33
Wind	$4 \cdot 10^6$	0.2
γ_{inj}	2.4	
E_0, GeV	1.0	
f	0.5	

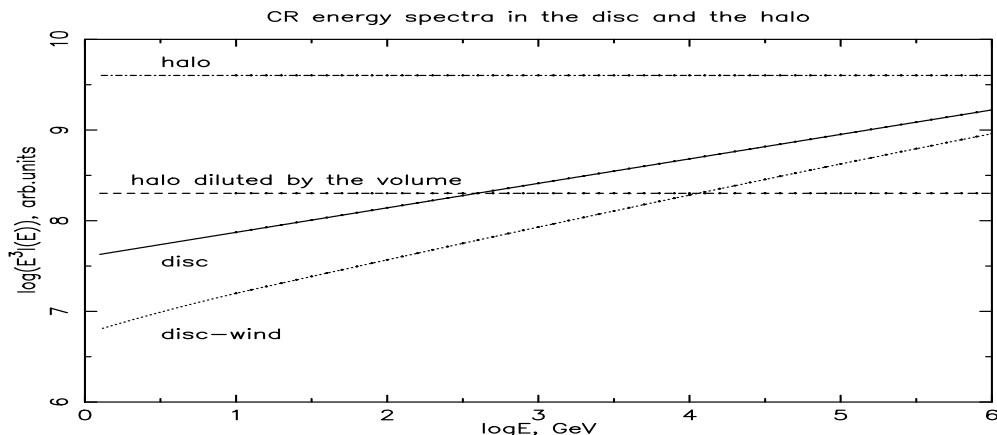


Figure 2: An example of the calculations illustrating the possible contribution of the Halo to the CR intensity: full line - Disc with no wind, dotted line - Disc with the wind, dashed line - Halo, dash-dotted line - CR intensity in the halo is diluted by the 20-fold larger volume.

Table 2. Numerical values of the parameters used, as an example, in the calculations shown in Fig.2.

It is seen that even for such a reasonable set of parameters shown in Table 2 and for the total number of particles in the Disc and the Halo it is impossible to reach a 20-fold excess of Halo over the Disc. If we take into account the large volume of the Halo (in Figure 2 it was assumed the cylindrical shape of the Halo with the tenfold increase of the vertical scale height) then the contribution of the GGH to the CR *intensity* (not the number of particles) at PeV energies will be only 10-20%. The wind cannot amplify the contribution of the Halo and reduce the amplitude of the anisotropy.

3.2.2 A non-standard propagation model

The amplitude of the anisotropy A is connected with the characteristics of the CR density N , its gradient $gradN$ and the diffusion coefficient D as $A = \frac{3DgradN}{cN}$, where c is the speed of light. In our propagation model $D(E) = H_d^2/\tau_d(E)$, where H_d is the vertical scale height of the Disc, which we assumed to be 1kpc and $\tau_d(E)$ is defined above as the lifetime of the CR particles in the Disc. Therefore,

$$A = \frac{3H_d^2 gradN}{cN\tau_d(E)} \quad (5)$$

This expression shows that there is a unique relationship between the mean CR lifetime $\tau_d(E)$ and the anisotropy A . Figure 3 shows the lifetime implied by our model (which has $\langle\tau_d\rangle = 4 \cdot 10^7 E^{-0.5}$ y with E in GeV) as given in Figure 1a with $\delta = 0.5$. Elsewhere, we have made predictions of the energy spectra using $\delta = 0.33$ [13] and others, eg [14] have made calculations for the same value of $\delta = 0.33$. Figure 3 shows three variants of the standard model.

Also shown, as 'NS', is the mean lifetime versus energy needed to give a best smooth line going through the experimental points in Figure 1a. It is seen that a dramatic

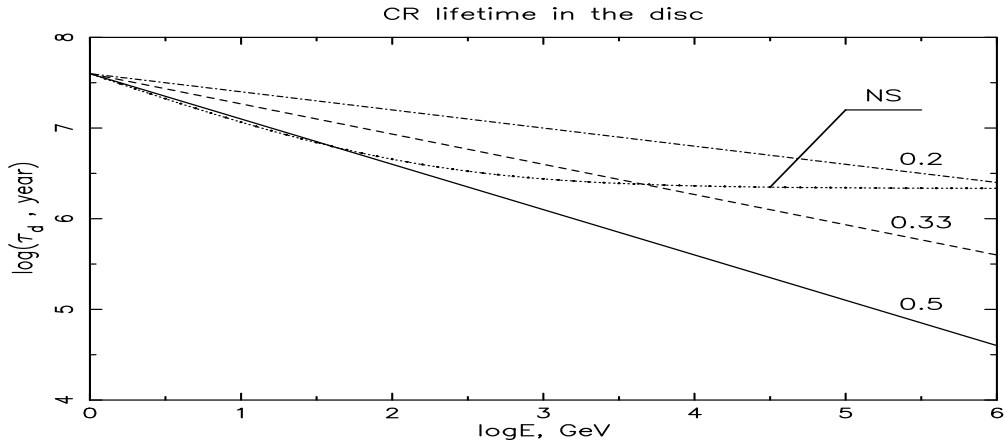


Figure 3: Lifetime τ_d vs Energy (protons, only, assumed) 'NS'is for non-standard propagation model needed to explain the observed anisotropy - the first harmonic amplitudes. Numbers at the other lines are values of δ - the exponent in the usual expression for mean lifetime vs energy: $\tau_d \propto E^{-\delta}$

flattening is needed above about $\log E, \text{GeV} = 3$. In fact, when allowance is made for a modest Halo [1] and downward fluctuations at the 10% probability level, $\delta = 0.2$ would suffice.

Consequences of the Non-Standard (NS) model are considered in some detail in the Appendix, but some general remarks are given here.

It has long been known that $\delta = 0.6$ is needed for $E \leq 100$ GeV/nucleon in order to explain the secondary to primary ratio (S/P) as a function of energy [16]. At higher energies smaller values of δ (0.3 to 0.5) have been commonplace. Indeed, in our own work [17] involving 'anomalous diffusion' values in the range $0.25 < \delta < 1.0$ were considered. There is thus a precedent for considering small values of δ .

Figure 4 shows the anisotropy amplitude $\log A$ vs $\text{Log} E$ for 10 samples of the SNR space-time distributions calculated with the 'non-standard' (NS) lifetime of CR protons shown in Figure 3. It is seen that the rise of the amplitude with the energy seen in Figure 1a changed to a nearly constant value at rather low absolute level. The change of the gradient $\frac{\text{grad} N}{N}$ expected with the change of the diffusion coefficient does not compensate the reduction of the amplitude due to the change of the lifetime.

3.3 The phase of the anisotropy

Again, there is a reassuring consistency of the phases from the different experiments (Figure 1b). A slow change of phase is indicated, from a phase of 90° at $\log E, \text{GeV} = 2$ to about zero at $\log E, \text{GeV} = 5$.

As might be expected, at 'low energies' where the local conditions of ISM are relevant, the experiments indicate a more complicated anisotropy pattern than a simple first harmonic and this aspect is taken up in the next section.

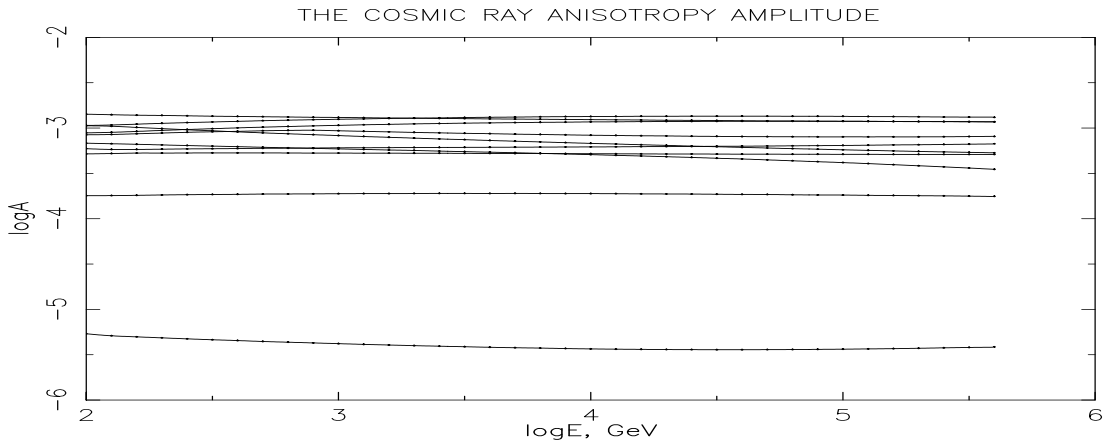


Figure 4: The anisotropy amplitude for 10 samples of SNR with the 'non-standard' propagation model.

3.3.1 Two-dimensional maps

The variation of the CR flux with the right ascension is better not analysed in terms of the simplified one-dimensional picture with the phase, often integrated over a large range of declinations. Rather one should examine the two-dimensional maps, provided by the publications, which often show a more complicated picture with a few excesses in different parts of the sky at different RA and δ . We are mindful of the potential criticisms of Andreev et al., 2008 [18] who criticise the validity of two-dimensional maps. Nevertheless, we continue to use the results of the experimenters themselves.

Figure 5 shows a schematic view of the location of CR excesses in both Equatorial and Galactic coordinates for the 5 new experiments, which published these maps: MILAGRO, ARGO-YBJ, Super-Kamiokande, IceCube and IceTop.

Positions of CR excesses observed in these experiments often split and overlap and we decided to give very schematic presentation of these excesses just to illustrate the location of the excesses in the CR sky. Contours of the ellipses in Figure 5 embrace very approximately the areas of excesses exceeding the mean background by three standard deviations. The upper half of Figure 5, panels (a) and (b) show maps in Equatorial coordinates, the lower half, panels (c) and (d) show the same maps in Galactic coordinates. Panels (a) and (c) show the excesses observed in the lower, 6 - 20 TeV energy domain. The overlap of the MILAGRO, ARGO-YBJ and Super-Kamiokande gives a measure of confidence for these measurements and confirms the puzzling conclusion made in [1] that in spite of the fact that the bulk of SNR, pulsars and other potential CR sources are in the Inner Galaxy surrounding the Galactic Centre, the excess of CR is observed in the opposite, Anti-Centre direction. The new point in these measurements is actually connected with the fact that MILAGRO and ARGO-YBJ collaborations observe two excesses in the same direction of the Anti-Centre, but both in the Northern and in the Southern Galactic Hemisphere. This gives an argument in favour of the conclusion that the CR at TeV energies originate in sources whose directions span a large range of Galactic latitudes.

The measurements of IceCube at the higher energy of ~ 20 TeV show that presum-

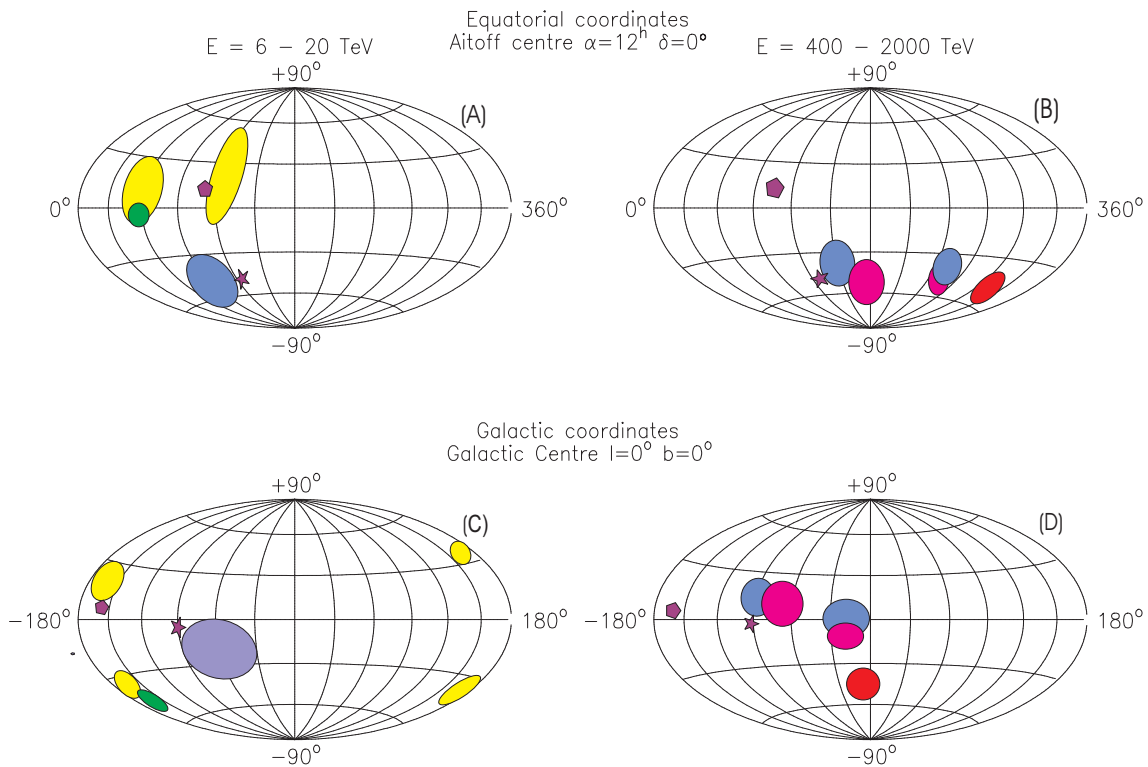


Figure 5: Schematic maps of CR excesses in Equatorial (a,b) and Galactic (c,d) coordinates for two energy domains: 6 - 20 TeV (a,c) and 400 - 2000 TeV (b,d). Excess regions observed in MILAGRO and ARGO experiments nearly overlap and are shown in yellow. Super-Kamiokande - green, IceCube - blue, IceTop - magenta for 400 TeV CR, red for 2000 TeV. The dark pentagon indicates the position of the Monogem Ring SNR, the dark star - the position of Vela X.

ably the excess region shifts in the direction of the third and fourth quadrants.

It would be expected that at tens of TeV energies the giroradius of particles in the typical magnetic fields of a few microgauss should be very small, ~ 0.01 pc. The diffusion of particles is thus strongly dependent on very local phenomena: the direction of the local regular magnetic field component, 'modulated' by the random field and the near-absence of a gradient of the CR density. The latter is determined by the influence of the 'Local Fluff' and the spiral Orion Arm which are located in the direction of the Outer Galaxy and can overcome the influence of the background CR flux from the sources in the Inner Galaxy [19]. The Local Fluff is a well known and important feature of the local ISM (see reference [19] for the original reference; much later work has confirmed the identification). It is of about 10 pc extent and can clearly affect the propagation of low energy CR, i.e. those of scattering length of this order and less. The effect will be significant in view of the fact that there will be transit time and, thereby, intensity differences from nearby sources depending on direction.

Inspection of Figures 1b and 5a,c shows that the value of ϕ is close to that expected for an excess of CR intensity from along the B -direction over the 'local' B -direction, the best fit being with the very local B -direction but the uncertainty in the actual values (typically $\pm 20^\circ$), and the likely effect of local field irregularities make the discrepancy understandable. Another important aspect is the gradient of the CR energy density

that would be expected in the absence of regular field effects. The near constancy of amplitude and phase indicates that the 'true' anisotropy (i.e. that which would occur in the absence of a regular field component) is very small.

The direction to the Galactic Anti-Centre from which the excess of CR arrive, as has been already remarked, is presumably due to factors connected with the small Galactocentric gradient of CR emissivity [20]. In that work it was suggested that shear in the ISM in the relatively undisturbed parts of the Outer Galaxy ISM was responsible for the (near-) lack of gradient. This would be in addition to the random nature of the SNR sources.

A further factor is that the reentrant PeV particle from the GGH will, themselves, have a small anisotropy from the general direction of the Galactic Centre.

4 Interpretation of the anisotropies above $\log E = 5$

Figure 1 and panels (b,d) of Figure 5 show results of anisotropy measurements at the relatively high energies of about 400 - 2000 TeV. They were made by two independent detectors: IceCube and IceTop at the South Pole. It is seen that the amplitude of the anisotropy, after falling down to the minimum at several hundred TeV, started to rise again above ~ 400 TeV, exceeding the value of $A \approx 10^{-3}$ in the PeV region.

The phase of the first harmonic dropped by nearly $150^\circ - 180^\circ$. An inspection of the two-dimensional map shows that the results of two measurements at the comparable energy of 400 TeV partly overlap, giving support to each other. The excesses observed at this energy occupy the region close to Galactic Disc in the fourth quadrant. At the highest energy of 2000 TeV IceTop experiment observed that the excess moved to the direction still closer to the Galactic Centre, but shifted to higher Southern Galactic latitudes.

At PeV energies the scattering length approaches 100pc and it would be expected that the influence of the local environment would become smaller and more distant regions of the Galaxy enter the scene. At larger distances from the solar system the higher density of sources in the Inner Galaxy overcomes the influence of the local environment and the CR excess moves toward the direction of the Galactic Centre. However, the existence of the knee and other fine structures in the CR energy spectrum give evidence that non-uniformity in the space-time distribution of sources still reveals itself at PeV energies and above.

Figure 5 shows the positions for the potential sources: the Monogem Ring SNR and Vela X pulsar with its pulsar wind nebula. The latter is young and can be a potential source if the particles can escape from the SNR associated with them. It is seen that both sources are in the Outer Galaxy and close to the Galactic Disc. The Monogem Ring SNR is nearby one of the excess regions indicated by MILAGRO and ARGO-YBJ at lower 6-20 TeV energies. It is not far from the direction towards the Anti-Centre and can in principle contribute to this excess. Counterargument that the excess area does not cover the position of the Monogem Ring SNR centre can be overcome by the fact that this SNR has a rather large size with a ring diameter of about 18° [21]. So we cannot reject the possible contribution of the Monogem Ring SNR to the anisotropy at

energies below 0.1 PeV on the basis of just anisotropy arguments. On the other hand, if the Monogem Ring is responsible for the knee and has rather flat energy spectrum, its contribution at energies below 0.1 PeV is negligible. Another worry is that this SNR cannot be associated so far with any excess at the higher 400-2000 PeV energies, although it has to be remarked that all the indicated measurements in panel (b) of the Figure 5 have been made at the South Pole and do not cover the positive declinations where the Monogem Ring is situated.

Vela X can in principle have relevance to the formation of the excess observed by the IceCube experiment in both energy domains. However, it is not in the direction of the Galactic Centre, but just close to the border between the third and fourth quadrants.

As for its characteristics as the potential CR source, not only is there the problem of particle escape from the encompassing SNR but the time window for emission of particles of adequate energy is not clear. This lack of clarity arises because of uncertainty about the pulsar's period at birth P_0 , its' past rate of energy loss and the efficiency for CR acceleration. A literature survey yields a range of P_0 : 18 to near 89ms. For most of the range, however, there should be an adequate window for PeV particles to be generated and the diffusion time from pulsar to the Earth is acceptable. The remaining questions relate to CR efficiency and particle escape.

5 Comparison with other work

Since the anisotropy is very small the work in this field is difficult because it requires high statistical accuracy. That is why the experimental data on the anisotropy at sub-PeV and PeV energies are rather poor. The KASCADE experiment did not find any anisotropy [22] and we give their upper limits in this and our previous paper [1].

Updated EAS-TOP data give only the amplitude and phase of the first harmonic [11] and not two-dimensional maps of the excesses in the CR flux. We used their data in our Figure 1.

In addition to our earlier work on the single source others have contributed to the development of the idea. Mention has already been made (in §1) of the work of Sveshnikova et al. [3] in which both known and simulated nearby SNR were considered. The dip in Figure 1a was not reproduced. Vela X was discounted because of the wrong phases above $\log E, GeV = 5$ appear not to have been included. Nevertheless, the work mentioned adds to the attention given to the role of the anisotropy as well as CR energy spectrum in defining a (possible) single source. Other workers who have developed our stochastic source distribution model include [14] and [23]. The idea of a 'non-standard model' was not mentioned, however.

Mention should also be made of very recent work [24]. The authors have claimed that heliospheric effect may be responsible for part at least of the anisotropy to energies as high as 100 TeV. This is a remarkable result insofar as heliospheric effects are usually considered to be small by 1 TeV. Confirmation, or otherwise, is awaited. In any event, our conclusions, and those of others, should not be affected beyond $\log E, GeV = 5$ where the case for the effect of a single nearby source is made.

6 Conclusions

Up to $\log E, \text{GeV} \sim 5$ there is consistency in the measurements of large scale (first harmonic) anisotropies and near constancy of phase: an important result enabling detailed analysis to be worthwhile. Transport along the 'local' magnetic field lines seems a likely cause although the direction of flow - from the general direction of the Galactic Anti-Centre - is surprising. The random space-time configuration of CR sources with the contribution of a few sources such as the Monogem Ring and Vela X SNR can play a role in the formation of the excess CR flux from the general direction of the Galactic Anti-Centre. A Giant Galactic Halo is inadequate to account for the comparatively small measured anisotropy. Another discrepancy to be explained is the lack of convexity in $\log A$ vs $\log E$ plot in our 'conventional model'. Instead, a new model is invoked: a 'Non-Standard' propagation model. Its acceptance, or otherwise, awaits further analysis.

Continuing with 'low' energies ($\log E, \text{GeV} \leq 5$), there is no obvious rapid change of the anisotropy with $\log E$, as yet. The 'New Component', claimed by us [25] from observations of the detailed spectral shapes of many elements might be expected to give a change of anisotropy amplitude/phase at 100 GeV. Unfortunately, this is just the lower limit for our study, and, in any event, solar modulation causes distortions below about 100 GeV. There are no features in the energy range $\log E, \text{GeV}$: 2 to 5 which can be attributed to fine structure (although there is an interesting hint of a decadal periodicity of phases with respect to $\log E$).

At higher energies there is evidence for a change in anisotropy amplitude and phase, although the experimental data are, as yet, rather sparse and cover mostly the area of negative declinations. They indicate that the amplitude of the first harmonic begins to rise with the energy and the phase changes to the opposite. The CR flux excess in Galactic coordinates shifts to the fourth quadrant and at the highest PeV energies to the direction of the Galactic Centre. An explanation in terms of the onset of a significant contribution from the sources in the Inner Galaxy and some of the local sources is promising. Although the Monogem Ring SNR is still possible, Vela X is a distinct possibility if its birth period were short enough ($P_0 \simeq 60\text{ms}$) and the particles were able to penetrate the surrounding Vela SNR envelope.

Acknowledgements

The authors thank the Kohn Foundation for supporting this work.

Appendix. A non-standard propagation model

It is shown in Figure 3 that the form of the $\log(\tau_d)$ vs $\log E$ dependence is non-standard, in the sense that it is not simple power law, in contrast with the usual assumption. In fact, as remarked already, the assumption of a unique, energy independent form of δ is simplistic: propagation of CR through the ISM is, no doubt, a process of great complexity.

In [17] varying degrees of turbulence were considered, giving rise, in turn, to varying degrees of anomalous diffusion (AD). Our adopted form of AD was characterised by the parameter α : 0.5 to 2.0, corresponding to $\delta = \frac{\alpha}{2}$ from 0.25 to 1.0. The lower the value, the greater the degree the degree of AD. Thus, Figure 3 indicates the need for

anomalous diffusion becoming more and more important as the CR energy increases.

The cause of this increase in anomalous diffusion is not immediately apparent. It would appear that higher energy particles sample parts of the Inner Galaxy (where the turbulence is bigger) to a greater degree than those of lower energy. In turn, this suggests that the scale height increases with energy, in distinction to the usual assumption of energy independence. The solution may lie in the model in which particles spiral around field lines and transfer from one line to another before joining a line that leads to escape from the Galaxy. The transfer probability may be energy dependent. The conventional diffusion model itself is not without problems, in that CR are assumed to diffuse until they reach a height where they immediately escape; such a model is, again, simplistic. The conventional Galactic Wind may have a role to play, in that its effect is energy dependent. However, at TeV energies and above its effect would not be expected to significant.

Another aspect of the Galactic Wind may be relevant at energies approaching on PeV, however. This relates to the possibility of acceleration of particles at the termination shock, following [26]. Insofar as the mechanism sends energetic CR back towards the Galactic Disc the termination shock acts as 'a reflecting boundary'. This is just what is required in our NS model, although it must be pointed out that the energies considered in [26] are somewhat higher than those considered here.

Understandably, changing the lifetime of CR requires a change in the CR injection spectrum. Specifically, the injection spectrum will need to be steeper. We have adopted an exponent (γ_{inj} in $N(E)dE = CE^{-\gamma_{inj}}dE$) equal to 2.15 and this fits the observed proton energy spectrum for $\delta = 0.5$. Changing δ to 0.2, for example, would need $\gamma_{inj} = 2.45$, a value increasingly away from the standard $\gamma_{inj} = 2$ for Fermi acceleration in a SNR envelope.

However, help is at hand when consideration is given to the time sequence of acceleration in SNR. As we have shown [27] the higher energy particles achieve most of their energy at later times. Specifically, most of the CR of $\log E > 4$ are accelerated in the last 20% of the time of the expansion of the remnant (64 to 80 kyears in our model). Thus, a steepened injection spectrum would arise quite naturally if SNR were leaky at these late ages. In fact, inspection of the observed SNR shows that they are rarely spherical and leakage seems inevitable. This feature is particularly marked for those SNR in the Inner galaxy. A further fact of relevance is the inevitable spread in the maximum energies of CR from SNR, arising from the variety of total energies, ISM densities and magnetic fields.

Finally, it should be remarked that in this scenario the 'Single Source' will need to have been an energetic SNR which did not leak prematurely.

References

- [1] Erlykin A D and Wolfendale A W, The anisotropy of galactic cosmic rays as a product of stochastic supernova explosions, 2006, *Astropart. Phys.*, **25/3**, 183
- [2] Erlykin A D and Wolfendale A W, 1997, High energy cosmic ray spectroscopy . I. Status and prospects, *Astropart. Phys.*, **7**, 1
- [3] Sveshnikova L G, Strelnikova O N and Ptuskin V S, 2011, On probable contribution of nearby sources to anisotropy and electron spectrum of cosmic rays at TeV energies, 32nd Int. Cosm. Ray Conf., Beijing, **6**, 184
- [4] Kiraly P, Kota J, Osborne J L et al., 1979, Cosmic ray anisotropy and the local interstellar medium, *Nuovo Cim.*, **2/7**, 1
- [5] Lidvansky A S, Andreev Yu M, Dzhappuev D D et al., 2008, Direction and the magnitude of the anisotropy of cosmic rays of TeV energies, 30th Int. Cosm. Ray. Conf., Merida, **1**, 613
- [6] Guillian G, Hosaka J, Ishihara K et al., 2007, Observation of the anisotropy of 10 TeV primary cosmic ray nuclei flux with the Super-Kamiokande I detector, *Phys. Rev. D*, **75**, 062003
- [7] Abdo A A, Allen B T, Aune T et al., 2009, The large-scale cosmic ray anisotropy as observed with Milagro, *Astrophys. J.*, **698**, 2121
- [8] Di Sciascio G (for the ARGO-YBJ collaboration), 2012, ARGO-YBJ: status and highlights, arXiv:1210.2635
- [9] Abbasi R, Abdou Y, Abu-Zayyad et al., 2012, Observation of anisotropy in the galactic cosmic-ray arrival directions at 400 TeV with IceCube, *Astrophys. J.*, **746:33** (11pp)
- [10] Aartsen M G, Abbasi R, Abdou Y et al., 2012, Observation of cosmic ray anisotropy with the IceTop air shower array, arXiv:1210.5278
- [11] Aglietta M, Alexeenko V V, Alessandro B et al., 2009, Evolution of the cosmic ray anisotropy above 10^{14} eV, *Astrophys. J. Lett.*, **692**, L130
- [12] Gupta A, Mathur S, Krongold Y et al., 2012, A huge reservoir of ionized gas around the Milky Way: accounting for the missing mass ?, *Astrophys. J. Lett.*, **756**, L8
- [13] Erlykin A D and Wolfendale A W, 2001, Supernova remnants and the origin of cosmic radiation, *J. Phys. G: Nucl. Part. Phys.*, **27**, 941
- [14] Blasi P and Amato E, 2012, Diffusive propagation of cosmic rays from supernova remnants in the Galaxy II: anisotropy *J. Cosm. Astropart. Phys.*, **01**, 011
- [15] Blasi P, 2012, Origin of galactic cosmic rays, arXiv:1211.4799

- [16] Obermeier A, Ave M, Boyle P et al., 2011, Energy spectra of primary and secondary cosmic-ray nuclei measured with TRACER, *Astrophys. J.*, **742**, 14
- [17] Erlykin A D, Lagutin A A and Wolfendale A W, 2003, Properties of the interstellar medium and the propagation of cosmic rays in the Galaxy, *Astropart. Phys.*, **19/3**, 351
- [18] Andreev Yu M, Kozyarivsky V A and Lidvansky A S, 2008, Anisotropy of galactic cosmic rays and new discoveries in its measurements, arXiv:0804.4381
- [19] Paresce F, 1983, Structure of the local interstellar medium and the line of sight to α Oph, *Lett.to Nature*, **302**, 806
- [20] Erlykin A D and Wolfendale A W, 2011, The 'cosmic ray gradient' in the Galaxy, *Proc. 2nd Int. Cosm. Ray Workshop 'Aragats 2012'*, 16
- [21] Thorsett S E, Benjamin R A, Brisken W F et al., 2003, Pulsar B0656+14, the Monogem Ring, and the origin of the 'knee' in the primary cosmic ray spectrum, *Astrophys. J. Lett.*, **592**, L71
- [22] Antoni T, Apel W D, Badea A F et al., 2004, Large-scale anisotropy with KASCADE, *Astrophys. J.*, **604**, 687
- [23] Pohl M and Eichler D, 2012, Understanding TeV-band cosmic-ray anisotropy, arXiv:1208.5338
- [24] Desiati P and Lazarian A, 2012, Anisotropy of TeV cosmic rays and the outer heliospheric boundaries, arXiv:1111.3075
- [25] Erlykin A D and Wolfendale A W, 2012, A new component of cosmic rays, *Astropart. Phys.*, **35**, 449
- [26] Völk H J and Zirakashvili V N, 2004, Cosmic ray acceleration by spiral shocks in the galactic wind, *Astron. and Astrophys.*, **417**, 807
- [27] Erlykin A D and Wolfendale A W, 2002, Supernova remnants and the origin of the cosmic radiation: the electron component, *J. Phys. G: Nucl. Part. Phys.*, **28**, 359